Heat-Transfer Measurements in Partially Ionized Air

P. H. Rose* and J. O. A. Stankevics†
Avco-Everett Research Laboratory, Everett, Mass.

A number of theoretical and experimental studies have been published on convective energy transport in a high-temperature, partially ionized gas. Certain uncertainties have arisen, particularly because of effects of the surface material of the heat-transfer gage. This investigation applies a new technique to heat-transfer measurements in a shock tube at simulated flight velocities up to 50,000 fps. An infrared heat-transfer gage has been adapted to this experiment. The advantage of this gage is that the heat-transfer measuring element is a carbon surface in thermal contact only on an infrared transmitting window, and thus the gage output is electrically completely decoupled from the partially ionized gas. The difficulties of adapting the gage to the test requirements are described, as well as the calibration of the infrared cell output and response time characteristics of the measuring system. The response of the gage to the heating encountered in both shock-tube end wall and on a stagnation point of a model are discussed with emphasis on the identification of radiative heat-transfer effects. The heat-transfer data support the previous results of the authors, and the various gage surface materials used did not change the heat-transfer rates measured.

Nomenclature

C	=	specific heat
C_P	=	gas specific heat
h	=	enthalpy per unit mass
k	=	thermal conductivity
l	=	thickness
$Nu/(R_e)^{1/2}$	=	heat-transfer parameter
p	=	local pressure
Pr	=	Prandtl number, $C_p\mu/k$
Q	=	heat-transfer coefficient
$\dot{q}$	=	heat-transfer rate
R_N	=	nose radius of axisymmetric body
T	=	temperature
t	=	time
U_s	=	incident shock-wave velocity
x	=	length dimension in gage measured from interface of carbon and window material
ρ	=	mass density
σ	=	$(\rho_2 k_2 C_2/\rho_1 k_2 C_1)^{1/2}$, Eq. (2)

Subscripts

e	=	end wall
s	=	stagnation condition
w	=	wall
1	=	carbon layer
2	=	*IR* (infrared) transmitting window

Introduction

Accurate definition of the severity of the planetary entry problem has been made difficult by the complexity of performing experiments in this environment. Although several experimental studies[1–3] have indicated a general agreement of their measurements with the theoretical work of Fay and Kemp,[4] Pallone,[5] and Hoshizaki,[6] it has been pointed out that all of these measurements depended on a common technique, the platinum calorimeter of thick-film resistance thermometer. Experiments reported in Ref. 7 have indicated that results of considerable variance can be obtained by the simple expediency of changing the gage material of the calorimeter.

In this situation, it was felt that a completely independent measurement of convective heat transfer by a different experimental technique would be worthwhile in settling the uncertainties that have been raised by the preceding experimental facts. The infrared heat-transfer gage developed by Camac[8] appeared to be available to make this independent judgment. Not only does this gage measure heat transfer through a completely different sensor system, but it also has the added advantage of being able to assess the effects of surface materials without a change in the calibration of the instrument. This, of course, could be accomplished by coating the same carbon infrared emitting surface with metallic coatings of various elements, a process that does not change the infrared emission characteristics of the carbon.

This paper reports on experiments in which the infrared heat-transfer gage was adapted to measure stagnation-point heat-transfer rates on the spherical nose of a model. The experiments were performed in a 6-in.-i.d. arc-heated driver shock tube.[9] The existence of a homogeneous hot-gas sample of predictable conditions in this shock tube has been documented in Refs. 1 and 9. In the present experiments, the tube was used at a length of 30 ft and an initial pressure of 0.25 mm Hg of air.

The principle of the infrared heat-transfer gage has been discussed in detail by Camac.[8] The gage consists of a thin, but opaque, surface of carbon deposited in good thermal contact on an infrared transmitting window. This surface, which might be overcoated with metallic coatings of various elements, is exposed to the heat-transfer medium, while its rear surface is viewed through the window with a wide-angle optical system that is imaged on the infrared detector. The obvious advantage of this gage is the fact that it is electrically decoupled from the shock-heated gas, and consequently there is no mechanism by which the ionized gases can interfere with the gage output.

The purpose of the present experiment was to combine the infrared gage technique with the electric arc-heated driver shock tube to provide the confirmation of the previous work on convective heat transfer. The solutions found to the various experimental problems, such as gage response, gage opacity, system calibration, and analysis of the data are described briefly in the following sections.

Presented at the AIAA Entry Technology Conference, Williamsburg/Hampton, Va., October 10–12, 1964 (no preprint number; published in bound volume of preprints of the meeting); revision received May 18, 1965. This work was sponsored by the NASA Office of Advanced Research and Technology under Contract No. NASw 748. The authors wish to acknowledge many informative discussions with M. Camac and R. Feinberg and the able assistance of C. Saunders, Jr. in performing the experiments.

* Associate Director. Associate Fellow Member AIAA.
† Senior Engineer. Member AIAA.

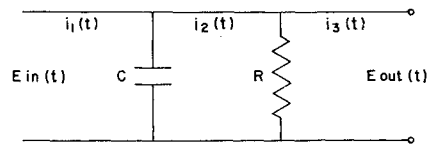

Fig. 1 Simplified infrared gage-amplifier-oscilloscope circuit.

Analysis of Gage Response

The temperature response of an infinite slab to an ideal heat-transfer pulse has been covered thoroughly in the literature;[10] a constant heat-transfer rate gives the familiar rise of surface temperature varying with the square root of time, and a heat-transfer rate decaying as $1/(t)^{1/2}$ gives the familiar jump to a constant elevated temperature. The infrared heat-transfer gage response to such an ideal heat-transfer pulse, including the fact that the infrared detector is imaged on the rear surface of the carbon layer while the heating occurs at the front surface, has been treated in detail by Camac.[8]

Two factors complicate the analysis further: 1) the gage system has a finite response time that, with extreme care, can be kept to about 1 μsec, and 2) the heat pulse imposed on the element is an odd combination of ideal pulses, i.e., one that decays inversely with the square root of time as the shock is reflected off the nose of the model and approaches the steady-state geometry, and, also, a constant heat-transfer rate pulse after the flow geometry has been established.

The interrelation of these three effects and their effect on achieving accurate heat-transfer measurements within the test time available has been investigated in some detail. For an arbitrary heat-transfer rate time history $\dot{q}(t)$, the convolution theorem gives the temperature response at the interface of a composite surface,[8] i.e., at $x = 0$, as

$$T(t, x = 0) = \int_0^t \dot{q}(t') T_\delta(t - t') dt \tag{1}$$

where $T\delta(t')$ is the temperature response to a δ function heat input at time $t = t'$. This temperature response can be written as

$$T_\delta(t, x = 0) = \frac{1}{(\pi k_1 \rho_1 C_1 t)^{1/2}} \frac{2}{(1 + \sigma)} \sum_{n=0}^{\infty} \left(\frac{1 - \sigma}{1 + \sigma}\right)^n \times \exp -(2n + 1)^2 \frac{l^2 \rho_1 C_1}{4 k_1 t} \tag{2}$$

Combining Eqs. (1) and (2),

$$T(t, x = 0) = \frac{2\sigma}{1 + \sigma} \frac{1}{(\pi k_2 \rho_2 C_2)^{1/2}} \int_0^t \frac{\dot{q}(t)}{(t - t')^{1/2}} \times \sum_{n=0}^{\infty} \left(\frac{1 - \sigma}{1 + \sigma}\right)^n \exp \frac{-(2n + 1)^2 \tau_1}{t - t'} dt' \tag{3}$$

where

$$\tau_1 \equiv l^2 \rho_1 C_1 / 4 k_1$$

For the case of the heat-transfer rate decaying inversely with the square root of time, i.e., $q = Q/(t)^{1/2}$, Eq. (3) can be shown to be numerically equal to the result used by Camac to show the effect of the thermal lag of the carbon layer, i.e.,

$$T(t, x = 0) = \frac{2}{1 + \sigma} \sum_{n=0}^{\infty} \left(\frac{1 - \sigma}{1 + \sigma}\right)^n \frac{Q\pi}{(\pi k_1 \rho_1 C_1)^{1/2}} \times \operatorname{erfc}\left(\frac{(2n + 1)^2 l^2 \rho_1 C_1}{4 k_1 t}\right)^{1/2} \tag{4}$$

The second effect that must be considered is that, although the temperature response of the interface is the desired quantity, the actual infrared gage output, as indicated on the oscilloscope, lags behind this quantity by the finite time response of the gage-amplifier-oscilloscope circuit. If we replace all of the circuit elements by a capacitance and resistance in the simple circuit, as shown in Fig. 1, then the problem is reduced to finding the accuracy with which $E_{out}(t)$ responds to its input $E_{in}(t)$. It can be shown that the current in the resistor R can be written as

$$i_3(t) = \exp -\frac{t}{\tau_2} \int_0^t i_1(t') \exp \frac{t'}{\tau_2} \frac{dt'}{\tau_2} \tag{5}$$

where τ_2 is the RC time constant of the circuit. If we assume that we are operating in a linear region of the gage output curve, i.e., T varies as E (which is only true approximately and over a limited temperature range), then the preceding equation can be written as

$$T_{out}(t) = \exp -\frac{t}{\tau_2} \int_0^t T_{in}(t') \exp \frac{t'}{\tau_2} \frac{dt'}{\tau_2} \tag{6}$$

Thus, even if the input to the IR gage were perfect, i.e., $T_{in}(t)$, the output would be degraded by the time constant of the system τ_2.

The third effect is a result of the complex heat pulse imposed on the model. When the incident shock arrives at the model, it reflects as it would off a solid end wall. The initial reflected shock velocity is known from the Rankine-Hugoniot equations, i.e., Ref. 11. At a shock velocity if 8 mm/μsec and an initial pressure of 0.25 mm Hg, the reflected shock will start at a velocity of 1.11 mm/μsec and would thus have a characteristic e-folding time to achieve its steady-state location of approximately 3 μsec for a body with a nose radius of 1.905 cm.

During these 3 μsec, the heat transfer to the body would be essentially that characteristic of an end wall of a shock tube, i.e., a rate decaying inversely with the square root of time. At some time, the three-dimensional effects will become dominant as the viscous boundary layer forms to its steady geometry, causing a constant heating pulse to the gage. This time has been estimated to be roughly the time required for a sound wave to reach the sonic point, i.e., approximately the nose radius divided by the stagnation sound speed. For the preceding conditions, this amounts to 6 to 7 μsec. Such times are in agreement with the times estimated for the

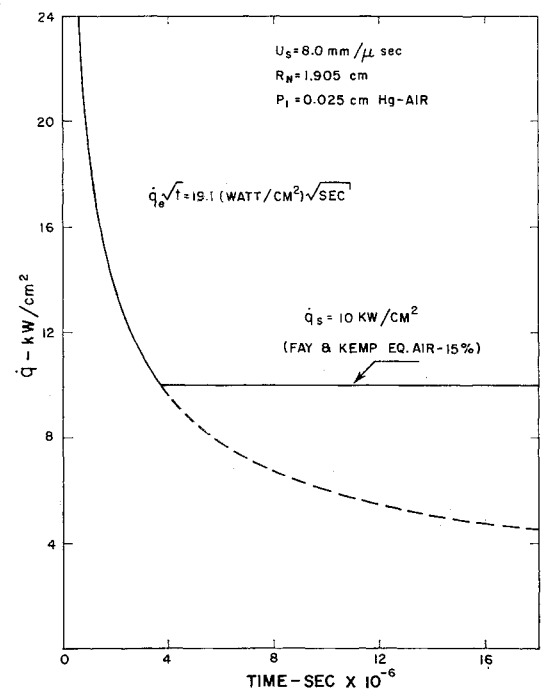

Fig. 2 Estimate of transient heat-transfer time history at the stagnation point of a spherical nosed body.

calorimeter heat-transfer gage output to reach a steady value.[1] Thus, a significant length of time is taken up by this process of setting up the steady flow geometry.

It is possible to estimate the expected heat-transfer rates during this transient period. We assume in calculating the heat-transfer history that the reflected shock flow geometry applies until the heat-transfer rate decreases below the value caused by a steady bow wave; after that a constant heat-transfer solution would be valid. For the end wall geometry, the heat transfer can be written as[12]

$$\dot{q}_e(t)^{1/2} = 0.88(k_w\rho_w/C_{pw})^{1/2}(h_e - h_w)[Nu/(Re)^{1/2}]' \quad (7)$$

where $[(Nu/(Re)^{1/2}]'$ is the value of $Nu/(Re)^{1/2}$ evaluated at the same stagnation pressure and enthalpy from stagnation-point boundary-layer calculations.[4] For the boundary-layer case, the equivalent expression is

$$\dot{q}_s(R_N)^{1/2} = \frac{1}{P_{rw}^{1/2}}\left(\frac{k_w\rho_w}{C_{pw}}\right)^{1/2}\left(\frac{2P_s}{\rho_s}\right)^{1/4}(h_s - h_w)\left[\frac{Nu}{(Re^{1/2})}\right] \quad (8)$$

It can be seen that the two expressions are almost identical except for the nose radius effect in the stagnation-point case that manifests itself in the stagnation-point velocity gradient term $1/R(p_s/\rho_s)^{1/2}$. The ratio of these two expressions gives a clue to which is the dominant one, i.e.,

$$\frac{\dot{q}_e}{\dot{q}_s} = \frac{P_{rw}^{1/2}0.88[Nu/(Re)^{1/2}]'}{(t/R_N)^{1/2}(2P_s/\rho_s)^{1/4}[Nu/(Re)^{1/2}]} \quad (9)$$

For the typical conditions of this experiment, the preceding ratio is very close to unity at times of a few microseconds, varying with t and R as indicated. The ratio of the Nusselts numbers is essentially 1, as the pressure and enthalpy do not vary greatly between stagnation and reflected conditions. The values of q_e and q_s are plotted in Fig. 2 for the specific case of $p_1 = 0.25$ mm Hg, $U_s = 8$ mm/μ, and $R_N = 1.905$ cm. At 1 μsec, q_e is 1.91 times q_s, whereas at about 3.6 μsec, the two are equal. For smaller bodies q_s would increase with $1/(R_N)^{1/2}$, and consequently the two would be equal earlier.

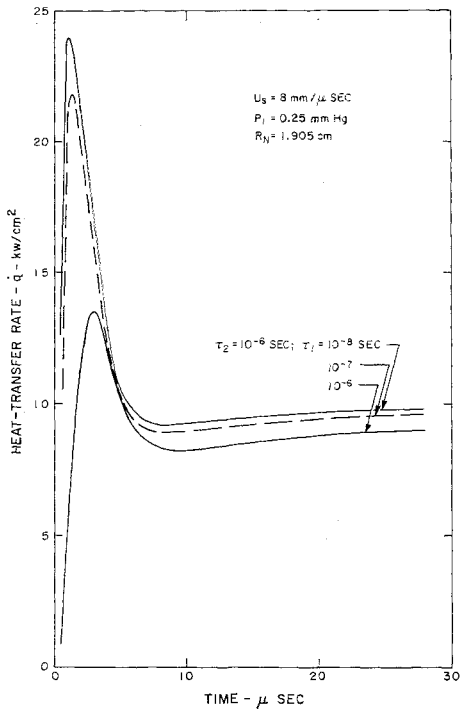

Fig. 3 Effect of thermal response of the window-carbon interface τ_1 on stagnation-point heat-transfer time histories.

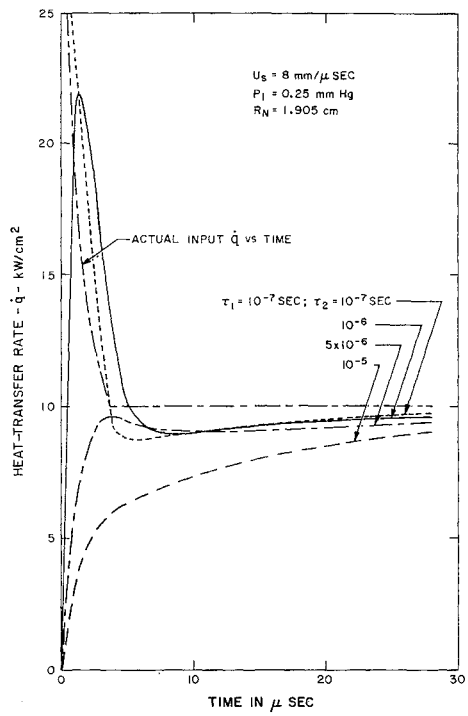

Fig. 4 Effect of infrared gage circuit response time τ_2 on stagnation-point heat-transfer rate time history.

Numerical experiments were performed to assess the requirements on the IR gage system to reproduce accurately the heating rates within the limit of test times available because of lag times of the carbon layer and circuitry. Using the heat-transfer time history shown in Fig. 2, we determined the temperature response of the window-carbon interface from Eq. (3) for various values of τ_1. This result can then be used as $T_{in}(t)$ to evaluate the effect of finite circuit response by use of Eq. (6) with various values of τ_2. The resulting $T_{out}(t)$ is representative of the signals, which are interpreted as the response to the gage to the heating in the actual experiments.

The final step in the numerical experiment is to subject the $T_{out}(t)$ in the usual manner used for reduction of transient heat-transfer data.[13] This is accomplished by solution of the inverted form of the heat condition equation, i.e.,

$$\dot{q}(t) = \left(\frac{k_2\rho_2C_2}{\pi}\right)^{1/2}\left[\frac{T(t)}{(t)^{1/2}} + \frac{1}{2}\int_0^t \frac{T(t) - T(t')}{(t - t')^{3/2}}\,dt'\right] \quad (10)$$

The resulting plots of heat-transfer rate, $\dot{q}$ vs time, give the degree to which the input data have been degraded because of various values of τ_1 and τ_2. A set of such results is shown in Figs. 3 and 4. It was concluded from these results that values of $\tau_1 \leq 10^{-7}$ and $\tau_2 \leq 2 \times 10^{-6}$ sec were tolerable under the experimental conditions.

This judgment is, of course, strongly tempered by the test times available in the experiment. If the transient phase consumes approximately 5 μsec, and the lags of the measurements are such as to spread this time into 10 μsec, it will be very marginal to make meaningful experiments in test times much less than 20 μsec. The performance of the shock tube used with respect to achievement of a uniform test gas has been discussed in Ref. 9 and is reasonably predictable from the work of Roshko.[14] At the conditions of the present experiments, average test times of 15 μsec are common. Thus, the 1- to 2-μsec criteria for the response of the gage system appeared critical.

If the resolution function of any given instrument is known a priori, then the measurement can, of course, be corrected after the fact for the degradation of information because of this resolution. For the case of the circuit response as shown in Eq. (6), this is a reasonable procedure and can be used to

lessen the criteria on the electronics. Equation (6) can be inverted by use of LaPlace transforms into a form where $T_{in}(t)$ can be expressed in terms of the measured $T_{out}(t)$ and the time constant of circuit τ_2 giving

$$T_{in}(t) = T_{out}(t) + \tau_2 dT_{out}/dt \qquad (11)$$

Equation (11) can thus be used to recover the original signal with some degree of accuracy. The experimental results were reduced by using Eq. (10) and then rechecked with the aid of Eq. (11), applying time constants of $\tau_2 = 1$ and 2×10^{-6} sec. The previous discussion of the difficulties of making accurate temperature measurements that, in turn, accurately reflect the heat transfer imposed on the surface is extremely important for shock-tube experiments in which the test times are very limited.

Experimental Techniques and Instrumentation

Adaptation of the infrared heat-transfer gage technique to the present experiments has involved the solution of several unique problems such as gage opacity, sensitivity, thermal adherence in the environment, dynamic calibration, and dynamic measurement of the gage response. The opacity requirement can be seen from the following simple considerations. The stagnation-point gases are of the order of 10,000°K–15,000°K. The contribution from this gas in the wavelength range of 1 to 10 μ is between 10^3 and 10^4 times as great as the signal from the carbon temperature rise, which is being measured. Thus, opacity means rejection of one part in 10^4 or better still 10^5. It was not possible to achieve this degree of opacity with only a carbon layer and yet maintain this layer thin enough to meet the response requirements. The addition of a metallic layer allowed fulfillment of the opacity requirement, although maintaining the fast response needed.

The sensitivity of the gage was optimized by the choice of window material, detector, and optical system. As a window material, magnesium oxide was chosen because of its optical characteristics. The radiation from the carbon layer that heats up to a maximum of 150°C during the experiment is predominantly in the 4- to 30-μ wavelength band. The Philco GPC 201 gold-doped germanium infrared detector cuts off at about 9 μ. The combination of this detector and window allows almost optimum transmission at wavelengths up to the capability of the detector.

Figure 5 shows the external transmission characteristics of magnesium oxide crystals (MgO 0, 50 mm thick) as used in this experiment. Magnesium oxide crystals show both good mechanical strength as well as infrared transparency at elevated temperatures up to 1000°C (Ref. 15). The fused MgO crystals, supplied by the Norton Company, were so-called "Magnorite."

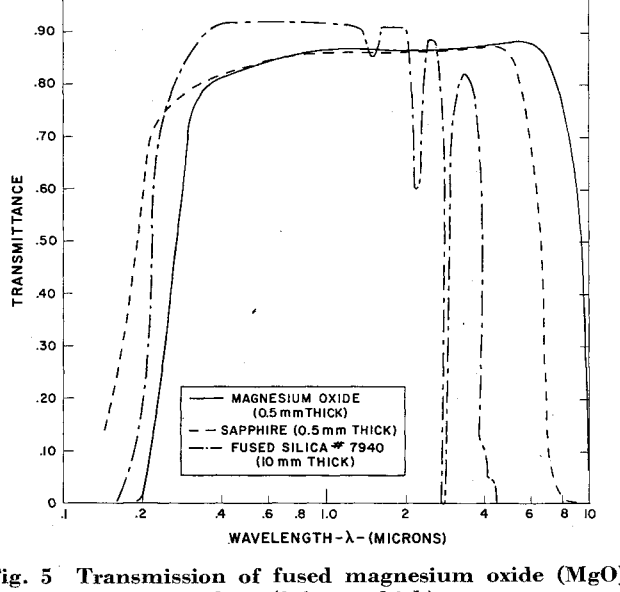

Fig. 5 Transmission of fused magnesium oxide (MgO) windows (0.5 mm thick).

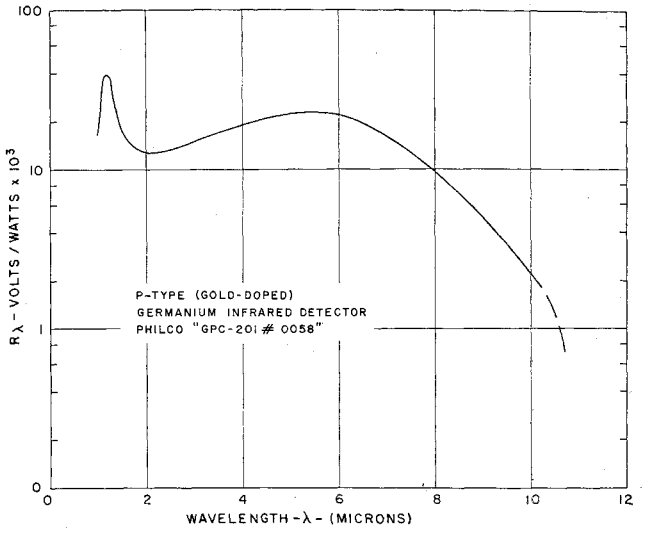

Fig. 6 Spectral responsibility of the Philco GPL-201 gold-doped germanium infrared detector used.

The infrared detector used in these experiments was the Philco GPC-201, a photoconductive, *P*-type, gold-doped germanium detector designed for operation at liquid nitrogen temperatures. Figure 6 shows the spectral responsivity of the infrared cell used in these experiments.

The optical system built into the model and test section is shown in Fig. 7. The sensitivity is optimized by the use of a Cassegrain mirror arrangement. By maintaining a spherical nose past the sonic point (approximately 40°), a larger-diameter mirror could be used to enhance the solid angle of the optical collector system. In some experiments, a phototube operating in the visible wavelength region monitored the light in the mirror system for evidence of transmitted light.

The deposition of sufficiently uniform, thin and adhering carbon layers on the MgO crystals was by chemical decomposition (pyrolysis) of methyl iodide CH_3I, as suggested by Camac.[8] The clean, roughened MgO window was then placed on a platinum strip, rough side up, into a vacuum bell jar containing a mixture of methyl iodide and helium. As an end product of this heated decomposition, we achieve a strong black layer of pyrolytic graphite on the MgO substrate. A carbon layer thickness of about 4000°–8000° Å is deposited in approximately 15 min which is opaque and measures optical densities between 5 and 8. (A unit of optical density is a factor of 10 in transmission measured at visible wavelengths.)

This method of deposition is assumed to produce pyrolytic graphite. The high degree of anisotropy in the structure of pyrolytic graphite results in thermal properties other than specific heat which are considerably different from commercial graphite. In calculating the response of the rear face of the carbon layer, as discussed in the previous section, the properties of pyrolytic graphite were used as reported in Ref. 16.

Overcoating the carbon layer with a metallic reflecting layer increases the thermal lag of the composite structure, increases the opacity, and changes the absorption characteristics of the surface. The latter has the effect of allowing convective heat-transfer measurements to be made in a radiating gas because most of the incident radiation can be reflected. The metallic layers, which were about 1000°–5000°Å thick, were vacuum-coated onto the carbon sublayers. This thickness of metal has a characteristic thermal diffusion time an order of magnitude less than the carbon, and thus the thermal response was not significantly affected. Uniform deposition of metallic

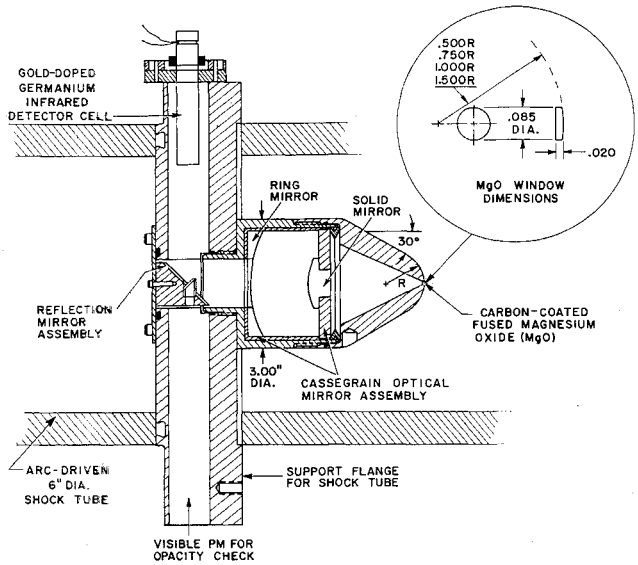

Fig. 7 Drawing of the infrared carbon gage, optical system, and detector built into shock-tube model.

films (aluminum, gold, copper, Nichrome) was obtained in Refs. 17 and 18. The surface of these coatings exhibited the characteristics of the carbon layers and appeared diffuse in reflectance.

For calculations of the thermal lag and heat capacity effects caused by the metal films, the bulk properties of the pure metal were used. However, it is known that the properties, particularly the strength, of thin films can vary significantly from the bulk properties.[18]

Calibration of the Infrared Gage System

The calibration of the infrared heat-transfer gage system consists of calibration of the absolute value of the output as well as the response. The former followed the procedure outlined by Camac[8] of replacing the shock-tube heat source by a blackbody heat source. A standard blackbody source was constructed in which a blackbody cavity was heated by well-agitated silicon oil through the temperature range of 0° to 190°C. A beam chopper placed in front of the blackbody source provides the AC method chopping at a frequency of 5000/sec. The emission of the chopper blade serves as the reference level as it is seen by the detector when the system is "closed." The output of the cell is fed through a standard cathode follower to an amplifier whose output is displayed on the oscilloscope.

In the shock-tube experiment, the heat-transfer gage senses a heating pulse of only 15 to 30 μsec duration. The temperature of the opaque layers rises up to 150°C during this time, but the MgO window remains essentially at room temperature. The calibration of the detector output for these short pulses can be evaluated by a series of four hypothetical measurements, as suggested by Ref. 8. Figure 8 shows the results of the two actual measurements required by this calibration procedure in terms of the infrared detector output plotted as a function of the temperature of the blackbody source. The highest output of the infrared cell V_1 occurs when the blackbody source is imaged directly on the detector. Here,

$$V_1 = V_B - V_c \tag{12}$$

where V_B is the voltage output caused by the blackbody source, and V_c is the signal caused by the temperature of the chopper wheel.

The lowest output curve V_2 in Fig. 8 is generated by the addition of the MgO windows to the holes in the chopper wheel. These windows degrade the transmission by the external transmission loss X averaged over the spectral sensitivity of the gold-doped germanium detector. These windows are, of course, at the chopper wheel temperature, which is essentially room temperature. This output V_2 is essentially

$$V_2 = X(V_B - V_c) \tag{13}$$

where the external transmission coefficient X is the result of combining the reflectivity at the two air-MgO interfaces r and the internal absorption of the MgO, α, as follows:

$$X = (1 - r)^2 e^{-\alpha x} \tag{14}$$

A third output could be generated if the MgO window is allowed to come to the temperature of the blackbody source, and thus the output of the detector will be V_1 degraded only by one single reflection loss at the MgO-air interface:

$$V_3 = (1 - r)(V_B - V_c) = V_1(1 - r) \tag{15}$$

A fourth output could be generated if the MgO window is coated by an opaque carbon layer, and the whole unit is maintained at the temperature of the blackbody source. The detector output can now be written as

$$V_4 = \left[\left(\frac{\epsilon X}{1 - r}\right) + \left(1 - r - \frac{X}{1 - r}\right)\right](V_B - V_c) \tag{16}$$

where ϵ is the emissivity of the carbon-magnesium oxide interface. Values of r of 0.065 ± 0.005 have been measured for MgO.

The first term in Eq. (16) represents the contribution of the emission from the carbon layer (degraded by transmission through the crystal and one reflection at the MgO-air interface), and the second term is the contribution caused by the radiation from the heated MgO windows.

For heat pulses of short duration, as are experienced in the present experiments, the only contribution that is observed is caused by the opaque layer. Almost all of the window remains at room temperature and makes no contribution. Thus, the short pulse becomes, in terms of the measured quantities,

$$V_G = \frac{\epsilon X}{1 - r}(V_B - V_c) = \left(\frac{\epsilon}{1 - r}\right) V_2 \approx \left(\frac{1}{1 - r}\right) V_2 \tag{17}$$

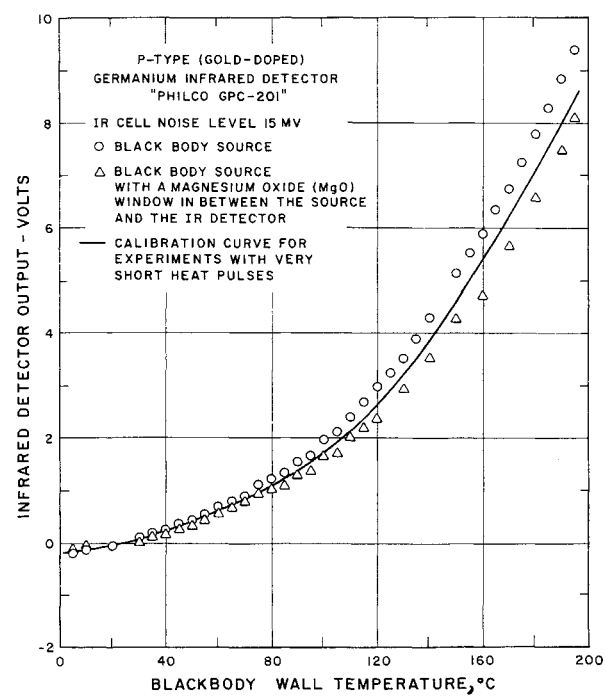

Fig. 8 Calibration curves of the infrared heat-transfer gage system.

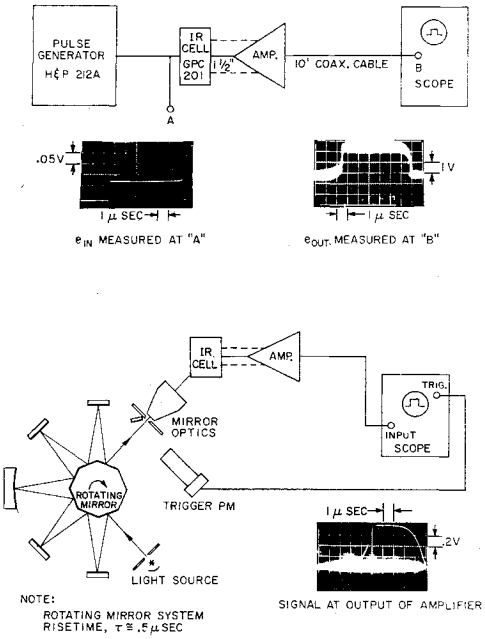

Fig. 9 Schematic diagrams of two setups used for measuring the time response characteristics of the infrared heat-transfer gage system, one using an electronic pulse and one a light pulse generator.

since the emissivity of the carbon-MgO interface is very close to 1. The curve-marked calibration curve in Fig. 8 is calculated from the previous equation.

From this calibration data, an empirical relationship between the calibration signal V_G and the blackbody temperature has been determined in the temperature range of 40° to 190°C. The data fit the following equation:

$$E(\text{volts}) = KT^n \tag{18}$$

with the constants $K \simeq 5 \times 10^{-5}$ and $n = 2.1 \pm 0.1$.

This calibration procedure has been checked against a dynamic calibration technique by a measurement of the end wall heat transfer in argon.[8,19] The correspondence of the semistatic (chopper wheel) and dynamic calibration has been assumed in these experiments.

In addition to the calibration of the infrared cell output previously discussed, the time response of the measuring system was determined. First, a pulse generator was used to impose an electronic pulse through the infrared cell and amplifier onto the oscilloscope. A schematic diagram of this calibration setup is shown in Fig. 9. The capacitance of the connection of the infrared cell to the amplifier is the critical parameter in determining the rise time of the system. By building the amplifier cathode follower and amplifier almost in a single integrated unit, it was possible to reduce the rise time of the system to slightly less than 1 μsec.

Another calibration was performed by the use of periodic light pulse generated by a rotating mirror system. The rise time of this light pulse itself was approximately 1 μsec. The resulting combination of the cell, amplifier, and light source gave a rise time of about 1.5 μsec.

The response time of the system was also tested by a heat-transfer test behind a reflected shock in the shock tube. A so-called knife-edge model was built for this purpose which replaced the hemispherical nose heat-transfer model shown in Fig. 7. This model is essentially an open tube aligned with the flow that holds the infrared gage and optical system in the same position as the other model but as part of a flat end wall geometry. The front of the tube is provided with knife edges so that the disturbances caused by the existence of these edges are isolated to the flow external to the tube. This model essentially slices a piece out of the test gas and allows the reflected shock to propagate back in the tube without external disturbances until it reaches the knife edge. Substituting the heat transfer for this geometry Eq. (7) into the equation for the interface temperature for this situation, i.e., Eq. (4), gives the familiar temperature step function response. Figure 10 shows the oscillograph from such an experiment. The rise time of this record shows the fast response (1–2 μsec) required of the gages and the approximately level output thereafter, indicative of the growth of the thermal boundary layer.

For stagnation-point heat-transfer experiments, the heat transfer starts out as in the preceding situation and then levels out at a constant value after the viscous boundary layer has been established. The oscillograms shown in Fig. 11 show this early heat-transfer time history clearly. As the example shows from the numerical calculation in the earlier section,

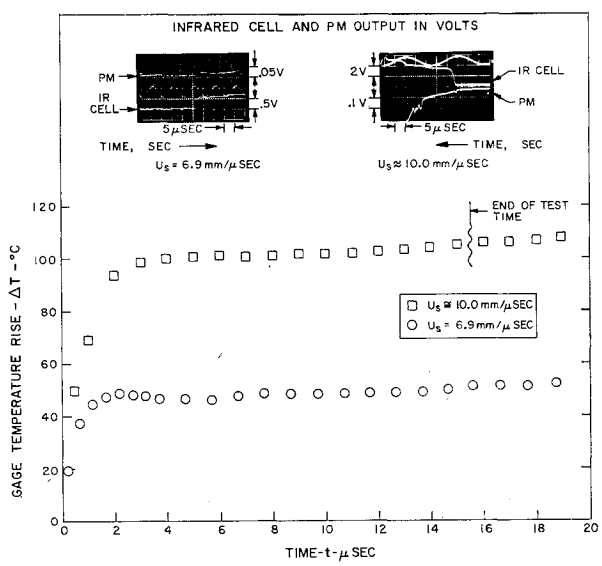

Fig. 10 Oscillograms of the data measured at two shock velocities with the infrared heat-transfer gage in the knife-edge model duplicating the shock-tube end wall.

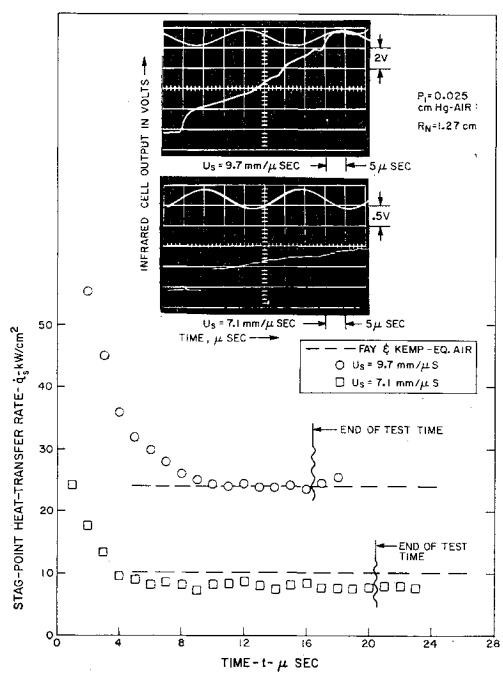

Fig. 11 Oscillogram of the data obtained at the stagnation point of the spherical nosed model measured with the infrared heat-transfer gage at two different shock velocities.

the temperature starts to rise when the flow geometry becomes established at times of the order of 8–10 μsec. For the constant heat-transfer input with time Eq. (8) the temperature response of the carbon-MgO interface is

$$T(t, x = 0) \sim \dot{q}(t)(t)^{1/2} \tag{19}$$

as can be seen from Eq. (3). If Eq. (18) is used as the calibration curve, then

$$E(t) \sim [\dot{q}KT^n]^{1/2} \sim \dot{q}^{0.5}t^{1.05} \tag{20}$$

or the output should be nearly linear with time with the slope being proportional to the square root of the heat-transfer rate. This characteristic is shown clearly by the oscillograms shown in Fig. 11.

The oscillograms shown have been reduced to heat-transfer time histories by use of the calibration curve Eq. (18) and the inversion formula Eq. (10). The heat-transfer time history is seen to indicate the characteristic discussed in the previous sections but settles down to a constant value well before the end of the test time, determined by monitoring the visible wavelength radiation with a photomultiplier.

As the infrared heat-transfer gage measures the temperature of the carbon layer on the surface of the MgO window during its exposure to the total environment, it responds to both convective and radiative heating, i.e., $\dot{q}$ (convective) + $\epsilon\dot{q}$ (radiative). But these two heating mechanisms could be differentiated since radiative heating is rejected quite efficiently because of high reflectance of the evaporated metallic films.[20, 21]

In the process of making the infrared gages, the metallic films were deposited on the chemically decomposed carbon layers that, in turn, were on a slightly roughened MgO crystal. The optical characteristics achieved by this process could well be considerably different from the literature values of evaporated films. In addition, it was also questioned whether the metallic surfaces deteriorated with time when exposed to ambient conditions.

The total reflectance of the various coatings was measured by a Beckman DK-2 (extended range) spectrophotometer,[22,23] useful over the wavelength range of 0.2 to 2.6 μ. The results of these measurements are presented in Fig. 12. It is clear that the plating procedure used degrades the reflectance somewhat but does not change the basic pattern of very high reflectance for metallic films and low reflectance for the carbon.

For the present series of experiments, the effect of radiative heat transfer was small. For the stagnation-point experiments, radiation merely manifests itself as an added increment of constant heat transfer $\dot{q}_{\text{rad}}$. As such, it is difficult to differentiate from the convective heating. Estimates of the magnitude of this effect are shown in Fig. 13, using Ref. 24 for the intensity of the radiative flux. It can be seen that, with an average surface emissivity of approximately 0.12 $\pm$ 0.05, it should be possible to keep radiative effects down to a maximum level of 5% below shock speeds of $U_s \leq 9.00$ mm/μsec. This is probably well within scatter of present experiments. Calculations based on recent work of Allen[25] at incident shock velocities greater than $U_s \geq 9.00$ mm/μsec indicate that the radiative heating could be larger than current estimates because of radiative contributions of lines and vacuum UV ultraviolet portion of the spectrum.

For the reflected shock geometry afforded by the knife-edge model, the radiative contribution is easier to isolate from the convective effects. Because of the growth of the thermal boundary layer, the convective heat-transfer rate falls inversely with the square root of time. The radiative heating will grow directly with time because of the increasing thickness of the radiating gas region, as long as the hot gas does not become opaque. A linear growth of the heating rate will result in a surface temperature increasing as the $\frac{3}{2}$ power of time and an infrared gage output rising approximately with time cubed.

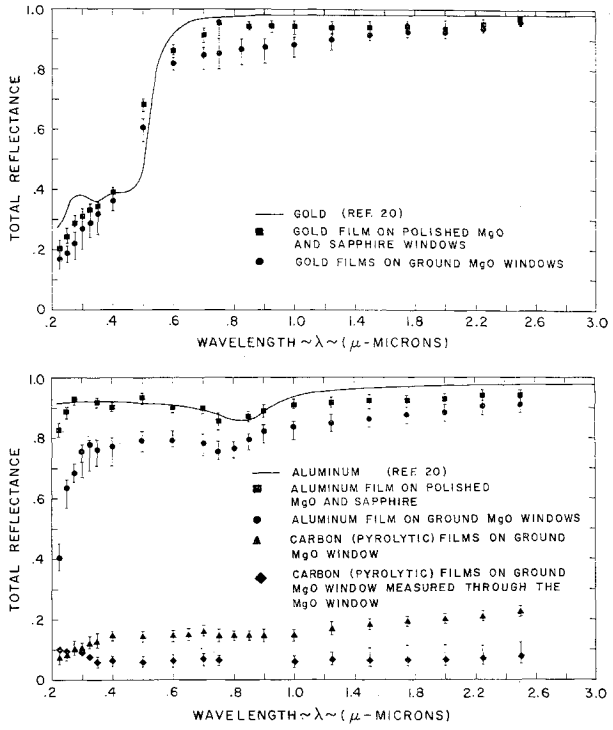

Fig. 12 Total reflectance measured for evaporated metal coatings deposited on the carbon layer on an MgO window.

Heat-Transfer Results

The heat-transfer data from the present series of experiments are shown in Fig. 14. The initial shock-tube pressure was 0.25 mm Hg, the gas was room air, and the incident shock wave velocities ranged from $U_s = 7$ to $U = 10.0$ mm/μsec, simulating[1] flight at altitudes of approximately 140,000 ft and a simulated velocity of up to approximately 50,000 fps. Only data points from experiments during which at least 8 μsec of test time were measured by one of the methods stated in Ref. 1 have been used in view of the response requirements discussed in the previous sections.

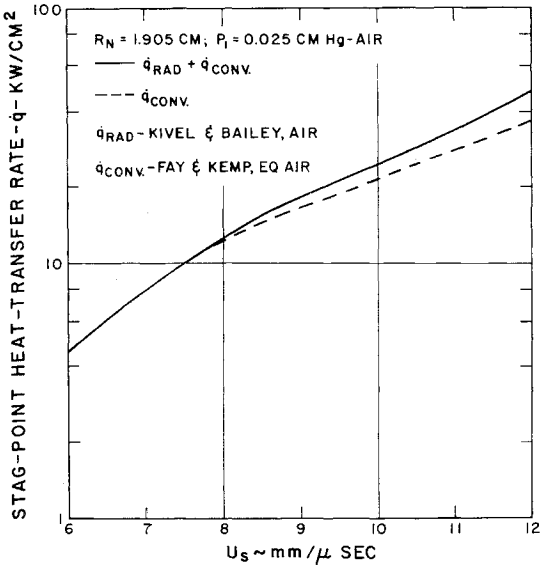

Fig. 13 Radiative and convective heating at the stagnation point of a model; convective heating was calculated from Fay and Kemp;[4] equilibrium boundary layer and radiative heating was computed from Kivel and Bailey,[24] assuming 100% absorption by the gage.

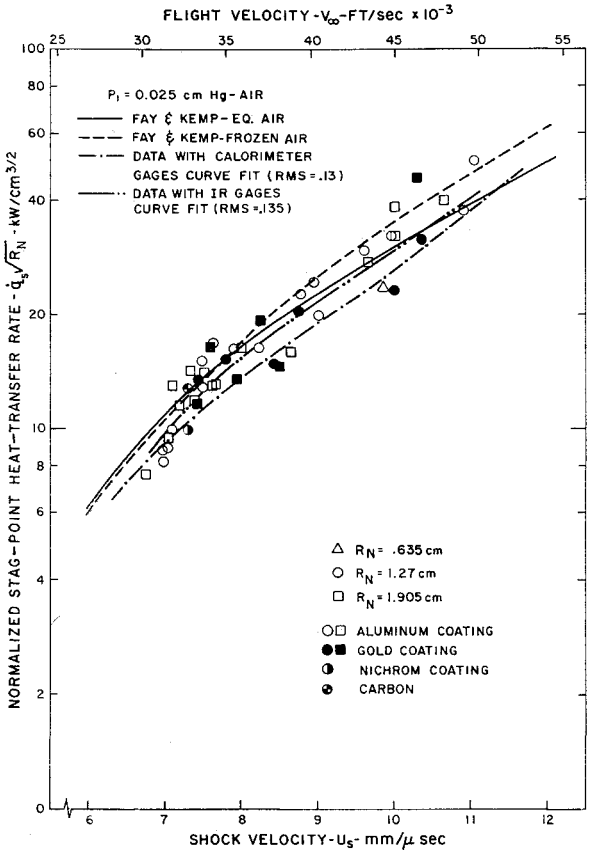

Fig. 14 Summary plot of stagnation-point heat-transfer rates measured with the infrared heat-transfer gage.

Stagnation-point convective heat-transfer data were measured mostly on sphere-cone models with nose radii R_N = 1.27 cm and R_N = 1.905 cm. The majority of the test runs were made with aluminum and gold reflective films overcoating the carbon gage. The infrared gage coatings lasted only for one shock-tube run and usually deteriorated after approximately 30 μsec, possibly because of impact of impurities and residues of the driver gas causing the film to become transparent. This was very plainly evident by the almost instantaneous rise of the signal beyond the range of the amplifier and scopes. The data have been compared with results calculated from the Fay and Kemp binary diffusion model for ionized diatomic gases.[4] Figure 14 also shows the curve fit of the data (which had an rms deviation of 0.13) obtained from measurements with calorimeter gages reported in Ref. 1. The present data appear to follow the theoretical predictions of equilibrium air somewhat more closely, and the majority of the data points thus lie slightly above the results of Ref. 1. The data obtained at shock velocities of $U_s > 10$ mm/μsec indicate an upward trend, also observed in Ref. 1, most likely caused by enhanced contributions of the *UV* radiative heating.[25]

There appears to be no significant difference between the data obtained with aluminum and gold films covering the carbon gage. This is in agreement with Collins and Spiegel[3] but in contrast to the result of gage material reported by Gruszczynski and Warren,[7] although their measurements were performed in N_2-CO_2 gas mixtures. Recent free-flight experiments reported in Ref. 26 also indicate the evidence that nickel gages do not lead to higher heating rates. In view of the fact that this investigation was performed at the lowest initial pressures used in any of these experiments, surface reactions should certainly have been present. The obvious advantage of this experiment over the previous references is that a single gage calibration is used for all of the surface materials, and, consequently, differences in the measurements, if present, could be directly attributed to surface gas interactions. Consequently, it must be assumed that the gage surface material does not have an influence on the convective heat transfer.

In this experiment, the test gas is assumed to be in equilibrium. These heat-transfer measurements must be viewed with the same reservations with respect to the state of the test gas, as discussed thoroughly in Ref. 1. Experimental measurements of the visible radiation show this to be a good assumption with respect to dissociation of the inviscid flow at the stagnation point. Our present knowledge of recombination rates indicates that the boundary layer may involve some freezing but not to a degree sufficient to influence the heat-transfer rate.[1] With respect to ionization, estimates and a discussion of the degree of completion of these processes were also made in Ref. 1. It was concluded that insufficient data on the ionization mechanism are available to make a very firm statement about the state of ionization, but arguments were put forth to support the assumption of ionization equilibrium. Recent experiments of Wilson[27] have tended to confirm these estimates. Wilson finds that behind strong shock waves the ionization mechanism in air is analogous to the process suggested by Petschek and Byron[28] for argon. Wilson finds that, in the air case, the initial ionization is provided by the atom-atom reactions (as by Lin)[29], and the impact process takes over as soon as sufficient electrons are produced. The result is that the time to achieve equilibration, in terms of the number of ambient mean free times, does not change radically even as the degree of ionization becomes significant, at shock velocities as high as 12 mm/μsec. This result confirms the extrapolations used in Ref. 1 and adds confidence to the assumption that ionization processes are in equilibrium in these experiments.

Summary and Conclusions

Heat-transfer measurements made with an infrared heat-transfer gage have been presented. The value of these measurements is that 1) a new technique has been developed for producing such measurements which is significantly different from the commonly used calorimeter resistance thermometer, 2) the measurements obtained with the new technique essentially duplicate and consequently verify the results of several authors achieved with calorimeter gages, and 3) variations of the surface material of the surface undergoing heat transfer did not alter the resultant heat-transfer rates showing conclusively that surface effects are not important under the experimental conditions.

References

[1] Rose, P. H. and Stankevics, J. O., "Stagnation-point heat-transfer measurements in partially ionized air," AIAA J. **1**, 2752–2763 (1963).

[2] Nerem, R. M. and Stickford, G. H., "Radiative and convective heating during hypervelocity re-entry," AIAA J. **2**, 1156–1158 (1964).

[3] Collins, D. J. and Spiegel, J. M., "Effects of gage material on convective heat transfer," AIAA J. **2**, 777–778 (1964).

[4] Fay, J. A. and Kemp, N. H., "Theory of stagnation-point heat transfer in a partially ionized diatomic gas," AIAA J. **1**, 2741–2751 (1963).

[5] Pallone, A. and Van Tassell, W., "The effects of ionization on stagnation-point heat transfer in air and in nitrogen," Phys. Fluids **6**, 983–986 (1963).

[6] Hoshizaki, H., "Heat transfer in planetary atmospheres at supersatellite speeds," ARS J. **32**, 1544–1552 (1962).

[7] Gruszczynski, J. S. and Warren, W. R., Jr., "Experimental heat-transfer studies of hypervelocity flight in planetary atmospheres," AIAA Preprint 63-450 (1963); also AIAA J. **2**, 1542–1550 (1964).

[8] Camac, M. and Feinberg, R. M., "High speed infrared bolometer," Rev. Sci. Instr. **33**, 964–972 (1962); also Avco-Everett Research Lab. Research Rept. 120 (March 1962).

[9] Camm, J. C. and Rose, P. H., "Electric shock tube for high velocity simulation," Phys. Fluids **6**, 663–678 (1963).

[10] Carslaw, H. S. and Jaeger, J. C., *Conduction of Heat in Solids* (Clarendon Press, Oxford, England, 1959), 2nd ed., pp. 55, 75, and 76.
[11] Feldman, S., "Hypersonic gas dynamic charts for equilibrium air," Avco-Everett Research Lab. Research Rept. 40 (January 1957).
[12] Kemp, N. H., "Approximate analytical solution of similarity boundary layer equations with variable fluid properties," Fluid Mechanics Lab., Dept. of Mechanical Engineering, Massachusetts Institute of Technology, Publication 64-6 (September 1964).
[13] Rose, P. H. and Stark, W. I., "Stagnation point heat transfer measurements in dissociated air," J. Aerospace Sci. **25**, 86–97 (1958).
[14] Roshko, A., "On flow duration in low pressure shock tubes," Phys. Fluids **3**, 835–842 (1960).
[15] Oppenhiem, U. P. and Goldman, A., "Infrared spectral transmittance of MgO and BaF_2 crystals between 27° and 1000°C," J. Opt. Soc. Am. **54**, 127–128 (1964).
[16] Garber, A. M., Nolan, E. J., and Scala, S. M., "Pyrolytic graphite—A status report," General Electric Co. Rept. R-63SD84 (October 1963).
[17] Holland, L., *Vacuum Deposition of Thin Films* (John Wiley and Sons, Inc., New York, 1960), Chaps. 1, 2, 5–7, and 11.
[18] Hass, G. (ed.), *Physics of Thin Films* (Academic Press Inc., New York, 1963), Vol. 1, Chaps. I and IV.
[19] Camac, M. and Feinberg, R. M., "Thermal conductivity of argon at high temperatures," J. Fluid Mech. **21**, 673–678 (1965).
[20] Gray, D. E. (ed.), *American Inst. of Physics Handbook* (McGraw-Hill Book Co., Inc., New York, 1963), 2nd ed.
[21] Gubareff, C. G., Janssen, J. E., and Torborg, R. H., "Thermal radiation properties survey," Honeywell Research Center Report, Minneapolis, Minn., 2nd ed. (1960).
[22] Trugillo, E. F., *Beckman DK-2 Ratio Recording Spectrophotometer Instruction Manual* (Beckman Instruments, Inc., Fullerton, Calif., 1962).
[23] Edwards, D. K., et al., "Integrating sphere for imperfectly diffuse samples," J. Opt. Soc. Am. **51**, 1279(1961).
[24] Kivel, B. and Bailey, K., "Tables of radiation from high temperature air," Avco-Everett Research Lab. Research Rept. 21 (December 1957).
[25] Allen, R. A., "Air radiation graphs: Spectrally integrated fluxes including line contributions and self absorption," Avco-Everett Research Lab., RN 561 (July 1965).
[26] Compton, D. L. and Cooper, D. M., "Some recent data on stagnation-point convective heat transfer in partially ionized air," AIAA J. **3**, 165–166 (1965).
[27] Wilson, J., "Ionization rates of air behind high speed shock waves," Avco-Everett Research Lab. Research Rept. 222 (to be published).
[28] Petschek, H. E. and Byron, S., "Approach to equilibrium ionization behind strong shock waves in argon," Ann. Phys. **1**, 270–315 (1957).
[29] Lin, S. C. and Teare, J. D., "Rate of ionization behind shock waves in air. II. Theoretical interpretation," Phys. Fluids **6**, 355–374 (1963).

SEPTEMBER 1965 AIAA JOURNAL VOL. 3, NO. 9

A Theorem Concerning the Stagnation Streamline in Potential Flow with Zero Circulation

JACK D. DENNON*
The Boeing Company, Renton, Wash.

Reasoning based on the physical mechanism involved in the potential flow rheoelectrical analogy has suggested a mathematical relation between the geometry of an immersed body and the remote location of the associated zero-circulation stagnation streamline. A theorem postulating this relation is presented, and an argument based on the theorem concludes that addition of a leading-edge flap to an airfoil will always produce an increase in the slope of the airfoil lift curve, and, for every airfoil at a given incidence, there exists a leading-edge flap that will maximize the potential flow lift.

Introduction

A DEVICE facilitating visualization of the remote ordinate of a streamline is best introduced at the outset. Consider two-dimensional potential flow past the arbitrary body shown in Fig. 1. Let a point A lie on the upstream branch of the stagnation streamline and a point B on the downstream branch. As points A and B are removed to locations sufficiently remote from the body so as to lie in the undisturbed stream, the straight line joining point A to point B will become parallel to the freestream. Such a straight line, which for brevity and suggestion has been given the name "stringline," may be generated for any streamline. The theorem to be presented is concerned with the stringline of a stagnation streamline in a flow with zero circulation about the body.

Received Novmber 12, 1964; revision received June 7, 1965. The potential flow lift calculations were performed by a computer program written by Franklin J. Davenport and Robert L. Palmer. Avtar S. Mahal has obtained similar data.

* Engineer, Airplane Division. Member AIAA.

Rheoelectrical Analogy

Streamlines in potential flow past an arbitrary two-dimensional body can be determined by the well-known electric-field mapping technique. Introduction of a model made of conductive material into an electric field that was initially uniform can be shown to produce a set of equipotential lines possessing a pattern that is the same as the pattern of streamlines in potential flow past a body of the same shape.

Suppose that a body of the shape shown by the dashed line in Fig. 2 is to be introduced into the electric field that (as shown by the straight equipotential lines) is presently uniform. The area to be occupied by the body is cut through by

Fig. 1 The straight line joining point A to point B becomes a "stringline" in the limit as both A and B move to remote locations.